atmosphere

MDPI

*Article*

# Prediction of Permafrost Subgrade Thawing Settlement in the Qinghai–Tibet Engineering Corridor under Climate Warming

**Jine Liu [1], Xiaona Liu [1], Jianbing Chen [2], Yue Zhai [1,*], Yu Zhu [1] and Fuqing Cui [1]**

[1] College of Geology Engineering and Geomatics, Chang'an University, Xi'an 710054, China; 2020026010@chd.edu.cn (J.L.); 2023226143@chd.edu.cn (X.L.); 2021126128@chd.edu.cn (Y.Z.); cfq731@chd.edu.cn (F.C.)

[2] National Key Laboratory of Green and Long-Life Road Engineering in Extreme Environment, CCCC First Highway Consultants Co., Ltd., Xi'an 710065, China; chenjianbing@ccccltd.cn

* Correspondence: zy@chd.edu.cn; Tel.: +86-13892833922

**Abstract:** As a result of global warming, the thawing settlement disasters of permafrost in the Qinghai–Tibet Engineering Corridor (QTEC) have intensified, which has serious effects on the safe operation of permafrost highway engineering. In this work, a prediction model for the thawing depth of permafrost subgrade in the QTEC under the climate warming scenario was established. Based on the survey results of permafrost ice content along the QTEC and the classification of thawing settlement risks, the zoning characteristics of thawing settlement of permafrost subgrade in the QTEC were obtained and analyzed. The results showed that the thawing depth of permafrost underlying the 26 m width subgrade in the QTEC will mainly remain below 9 m, and the area with a thawing depth of 6~9 m will have the widest spread within the next 20 years. The thawing settlement will be between 0.02 m and 5.45 m, with an average value of about 0.93 m after 20 years. Furthermore, after 50 years, the thawing depth of permafrost underlying the 26 m width subgrade will almost always be greater than 9 m, and the average thawing settlement will be about 1.12 m. Within the next 20 to 50 years, the risk of permafrost subgrade thawing settlement in the QTEC will be the most significant risk type, and this effect will mainly be distributed in the Kunlun Mountains, Chumar River Plain, Kekexili Mountains, Beiluhe Basin, Tanggula Mountains and intermountain Basins.

**Keywords:** climate warming; Qinghai–Tibet engineering corridor; permafrost subgrade; thawing settlement; regional characteristics

check for updates

**Citation:** Liu, J.; Liu, X.; Chen, J.; Zhai, Y.; Zhu, Y.; Cui, F. Prediction of Permafrost Subgrade Thawing Settlement in the Qinghai–Tibet Engineering Corridor under Climate Warming. *Atmosphere* **2024**, *15*, 730. https://doi.org/10.3390/atmos15060730

Academic Editors: Ruiqiang Bai, Jiwei Wang and Xiao Jin

Received: 15 May 2024
Revised: 16 June 2024
Accepted: 17 June 2024
Published: 19 June 2024

**Copyright:** © 2024 by the authors. Licensee MDPI, Basel, Switzerland. This article is an open access article distributed under the terms and conditions of the Creative Commons Attribution (CC BY) license (https://creativecommons.org/licenses/by/4.0/).

## 1. Introduction

The Qinghai–Tibet Plateau contains a significant number of permafrost areas, comprising 70% of the permafrost area in China, and is highly sensitive to external thermal disturbances. With global warming and increasing human activities, the permafrost in the Qinghai–Tibet Plateau continues to degrade, inducing potential hazards to various permafrost engineering projects [1]. The QTEC starts from Golmud and ends in Lhasa, with a total length of 1100 km, crossing about 550 km permafrost areas, which is a lifeline connecting Tibet and Chinese inland areas [2,3]. However, highway engineering has disrupted the thermal equilibrium of the original permafrost environment and caused subgrade diseases such as frost heave and thawing settlement. Among the various kinds of highway disease, thawing settlement is the main form of subgrade damage present in the QTEC, and it is caused by the increasing temperature of permafrost strata and the subsequent consolidation drainage and compression of the molten layer [4,5]. Furthermore, according to the IPCC report, the average air temperature is expected to rise by 0.3 °C every decade throughout the 21st century, with a potentially greater increase in high-altitude areas [6]. Therefore, the stability of permafrost subgrade under the context of climate warming has attracted much attention from scholars. As temperatures rise, the problem of permafrost subgrade thawing settlement will intensify, so studying the future distribution

characteristics of thawing settlement in the Qinghai–Tibet Engineering Corridor is crucial for the construction and maintenance of permafrost subgrade stability.

Permafrost is highly sensitive to temperature changes, and in recent years, there has been a noticeable increase in thawing settlement. Scholars have begun to pay more attention to the prediction of permafrost subgrade thawing settlement and carrying out related research [7–9]. Deng et al. [10] developed a coupled model based on the Darcy–Stefan model and the theory of porous media elasticity to predict the permafrost thawing settlement, showing that the model could improve the calculation accuracy of thawing settlement. Chen et al. [11] organized permafrost subgrade observation data from 2010 to 2019 and analyzed the characteristics of permafrost deformation and noted a significant linear relationship between thaw settlement and time. Guo [12] proposed a subgrade thawing settlement prediction model based on the gray BP neural network in the Qinghai–Tibet Railway and predicted the hazardous areas of subgrade thawing settlement after three and ten years. Wang [13] proposed a method to calculate permafrost thawing settlement along the Beihei Expressway and predicted settlement under different working conditions. Zaretskii [14] studied the deformation of permafrost thawing settlement through experimental data and obtained a method with which to calculate the thawing settlement deformation by the ice content. Sun et al. [15] analyzed monitoring data in the Qinghai–Tibet Engineering Corridor from 1966 to 2018, established a transient moving network model of permafrost thawing settlement, and found that thawing settlement in ice-rich permafrost areas at zero degrees had a high risk. Ni et al. [16] analyzed the reliability of thawing settlement indices based on the geological disaster index and used a comprehensive optimization index to predict permafrost subgrade thawing settlement disasters in the Qinghai–Tibet Plain.

Currently, due to global climate warming, many scholars have conducted relevant studies to explore the characteristics of permafrost subgrade thawing settlement deformation under climate change [17–19]. Hong et al. [20] analyzed the characteristics of climate warming and permafrost subgrade thawing settlement to establish a Permafrost Settlement Hazard Index (PSHI) and found that discontinuous permafrost areas were more prone to thawing settlement, and that climate models could be used to predict the thawing settlement risk in 2050. Ruan et al. [21] established a modified thawing settlement index model, studied the future thawing settlement disaster risk under climate change in the Qinghai–Tibet Engineering Corridor, and further analyzed the zoning characteristics of future thawing settlement risks. Zhao [22] selected permafrost area at high temperatures as a research object, compared 31 climate models from the fifth phase of the Climate Model Intercomparison Project (CMIP5) to predict changes in near-surface air temperature, and assessed the permafrost degradation process using a thermal model. Heidi et al. [23] conducted the permafrost warming experiment in Alaska, using high-precision global positioning systems to quantify subsidence and identify its environmental driving factors, showing that the amount of thawing settlement increased fivefold from the baseline. Thawing settlement is influenced by permafrost characteristics such as the ground mean annual temperature, the active layer thickness and ice content. Zhang et al. [24], Xu et al. [25] and Nan et al. [26] analyzed the changes in permafrost characteristics under different climate change scenarios. Based on research from the 1980s on the division of permafrost and thawing zones in the Tuotuohe Basin, Wei et al. [27] used geothermal observation data from boreholes along the Qinghai–Tibet Railway to study the ground temperature and its changes in the permafrost and thawing zones. Previous studies have mainly focused on the deformation patterns and numerical predictions of subgrade thawing settlement but have rarely addressed the changes in subgrade thawing settlement in response to climate change. Thus, the present work proposed a predictive approach integrating GMAT, ALT and ice content factors for 26 m width permafrost subgrade thawing settlement. A numerical model for calculating GMAT and ALT while considering the climate warming effect was also developed. Then, the distribution characteristics of thawing settlement and risk level along the QTEC in the next 20 and 50 years were obtained and analyzed.

## 2. Methods

### *2.1. Calculation Method of Subgrade Thawing Settlement*

Along the QTEC, the geological environment is complex and the climate change varies greatly. The subgrade thawing settlement disease of permafrost is closely related to the ice content and subgrade thawing depth. High-ice-content permafrost is extremely sensitive to changes in hydrological conditions, the melting of underground ice will lead to surface subsidence [28,29] and the subgrade thawing depth reflects the degree of permafrost subsidence. We established a prediction model for the thawing settlement of permafrost subgrade in the QTEC under the climate warming scenario. The detailed research framework is presented in Figure 1.

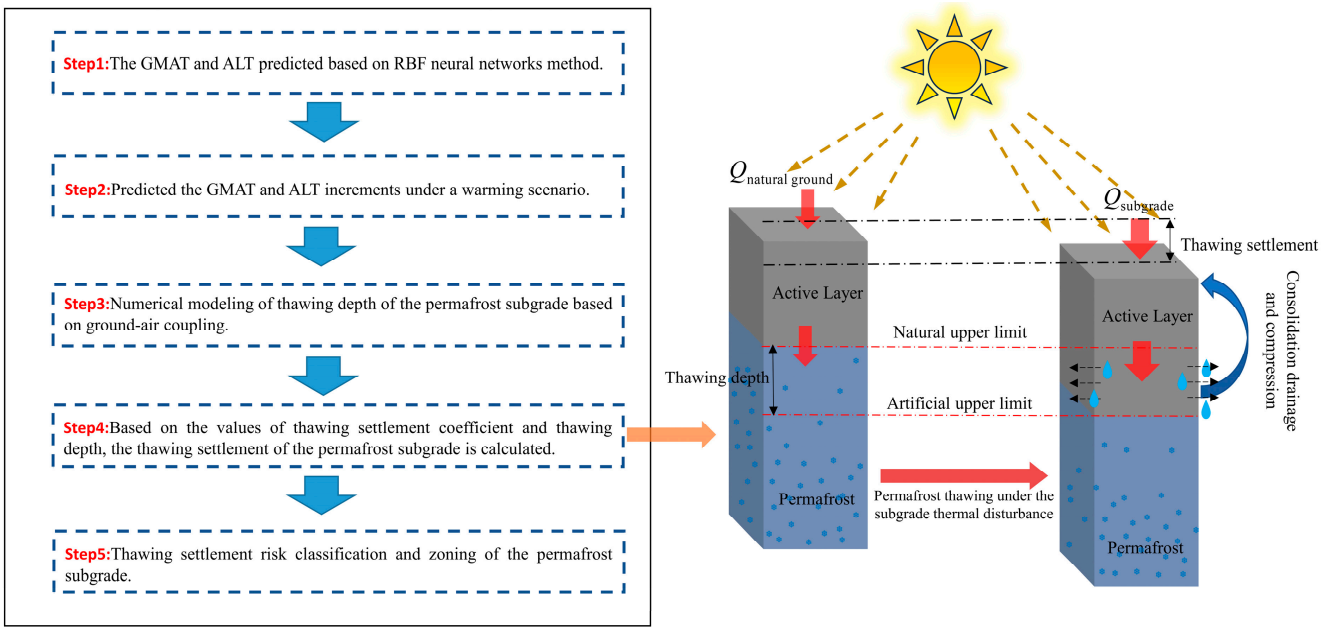



**Figure 1.** Research framework of permafrost subgrade thawing settlement.

The subgrade thawing settlement was calculated by combining the subgrade thawing depth and the subgrade thawing settlement coefficient, as follows:

$$I = \Delta h \times A \quad (1)$$

where $I$ is the subgrade thawing settlement (m); $\Delta h$ is the subgrade thawing depth (m); $A$ is the subgrade thawing settlement coefficient.

The value of the subgrade thawing settlement coefficient was determined by the ice content. According to the ice content characteristics of permafrost on the Qinghai–Tibet Expressway, it can be divided into five types: ice-poor, icy soil, ice-rich, ice-saturated and ice layer with soil inclusions [30]. The distribution of ice content in the QTEC was obtained by field drilling survey method. Utilizing the permafrost ice content survey results, the subgrade thawing settlement coefficient of permafrost along the QTEC was classified and valued [31], as shown in Table 1.

**Table 1.** Subgrade thawing settlement coefficient values of permafrost with different ice contents.

| Ice Content | Ice-Poor | Icy Soil | Ice-Rich | Ice-Saturated | Ice Layer with Soil Inclusions |
|---|---|---|---|---|---|
| Thaw settlement coefficient | 0.01 | 0.03 | 0.065 | 0.175 | 0.25 |

The thawing depth of permafrost subgrade is influenced by various factors such as surface conditions and vegetation environment. In the previous research results [31], a

calculation formula between the permafrost subgrade thawing depth and the GMAT and ALT was established by combining numerical calculation and radial basis function (RBF) neural networks methods. The distribution of GMAT, ALT, and subgrade thawing depth of permafrost in the QTEC was analyzed separately. The calculation formula for subgrade thawing depth was as follows:

$$\Delta h = 0.3167e^{3.8404\times(0.806+0.107T+0.036D)} \quad (2)$$

where $\Delta h$ is the subgrade thawing depth of permafrost (m); $T$ is the ground mean annual temperature (°C); $D$ is the active layer thickness (m). The goodness-of-fit $R^2$ of the subgrade thawing depth prediction model was 0.979, indicating a good fitting effect, and could accurately predict the permafrost subgrade thawing depth in the QTEC.

### *2.2. Prediction Methods for GMAT and ALT under Climate Warming*

To investigate the future variation of GMAT and ALT under climate warming, an earth–atmosphere coupled numerical model was established. The calculation model was composed of an air environment and a natural soil layer (as shown in Figure 2). To make the calculation results more general, the natural soil layer was simplified as a single soil property. At the same time, considering the distribution characteristics of the surface soil in the QTEC, the natural soil layer property was selected as the most widely distributed gravel soil on the surface based on the field survey results along the Qinghai–Tibet Highway [32]. The thickness of the soil layer was taken as 30 m. To reduce the influence of the upper wall boundary of the model on the calculation of turbulence in the air region, the height of the air layer was taken as 40 m. In addition, to avoid the influence of entrance effects on the calculation results, the length of the calculation model was taken as 120 m.

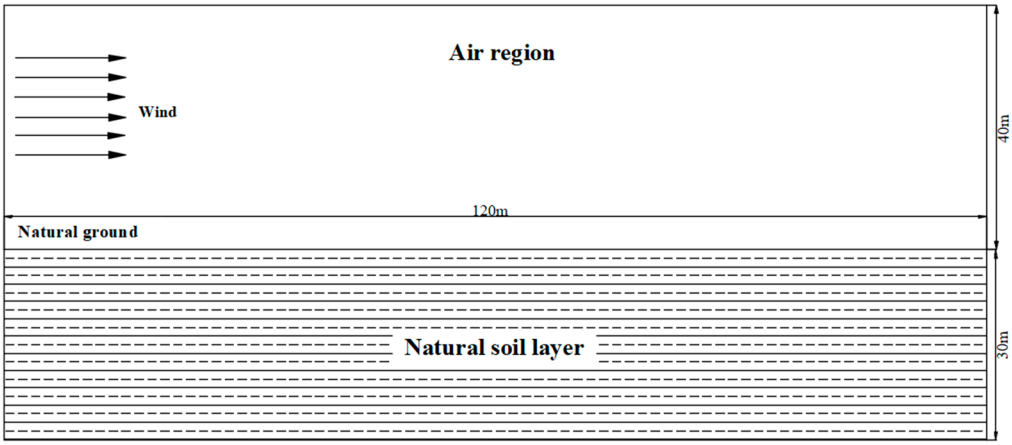



**Figure 2.** Earth–atmosphere coupled numerical model for GMAT and ALT calculation.

Numerical simulation was conducted on the GMAT and ALT changes under the condition of the air temperature increase of 0.022 °C/year. The numerical calculation was based on a two-dimensional unsteady turbulence model, and implicit algorithms were used for numerical solution. In the numerical calculations, the air environment above the natural ground was considered as a free fluid and the air was considered as an incompressible gas with constant density. The turbulence calculation was carried out using the standard $\kappa$-$\varepsilon$ model [33]:

$$\frac{\partial(\rho\kappa)}{\partial t} + \frac{\partial}{\partial x_i}(\rho u_i \kappa) = \frac{\partial}{\partial x_i}\left(\left(\eta + \frac{\eta_t}{\sigma_\kappa}\right)\frac{\partial \kappa}{\partial x_i}\right) + G_k - \rho\varepsilon \quad (3)$$

$$\frac{\partial(\rho\varepsilon)}{\partial t} + \frac{\partial}{\partial x_i}(\rho u_i \varepsilon) = \frac{\partial}{\partial x_i}\left(\left(\eta + \frac{\eta_t}{\sigma_\varepsilon}\right)\frac{\partial \varepsilon}{\partial x_i}\right) + \frac{\varepsilon}{\lambda}(c_1 G_k - c_2\rho\varepsilon) \quad (4)$$

where $\kappa$ is the turbulence pulsation kinetic energy; $\eta_t$ is the dynamic viscosity caused by turbulent fluctuation; $\sigma_\kappa$ is the Pr number of turbulence pulsation kinetic-energy; $G_\kappa$ is the produced items of turbulence pulsation kinetic-energy; $\varepsilon$ is the turbulent dissipation rate; $\sigma_\varepsilon$ is the Prandtl number of turbulent dissipation; $c_1$ and $c_2$ is the empirical constant.

The heat conduction of the natural strata was solved using the equivalent heat capacity method, which is controlled by equation [34]:

$$C^* \frac{\partial T}{\partial t} = \frac{\partial}{\partial x}\left(\lambda^* \frac{\partial T}{\partial x}\right) + \frac{\partial}{\partial y}\left(\lambda^* \frac{\partial T}{\partial y}\right) \quad (5)$$

where $C^*$ and $\lambda^*$ are the equivalent thermal capacity and equivalent conductivity, respectively.

The numerical calculations were performed using the ANSYS Fluent 15.0 software package. The physical properties of the air region were chosen as the air at 0 °C. The density of the permafrost layer was set to a constant value, and its specific heat capacity and thermal conductivity were taken as a temperature-dependent function of the segmental step type [35,36]. To reflect the impact of periodic changes in the external environment on coupled heat transfer of underlying permafrost, environmental temperature, wind speed, solar radiation, evaporation, etc., were all set as annual periodic change functions over time. The calculation time was set to 50 years, and the convergence standard for calculating residuals was uniformly set to $10^{-5}$.

According to the numerical calculation results of the permafrost GMAT, the linear fitting formula between the increase in GMAT after 20 and 50 years and the initial GMAT can be obtained as follows:

$$\Delta T = a + bT_0 \quad (6)$$

where $\Delta T$ represents the increase in GMAT after 20 and 50 years; $T_0$ is the initial GMAT; $a$, $b$ were the coefficients of the linear fitting formula, which is $-0.1339$ and $-0.1472$ after 20 years and $-0.0237$ and $-0.2537$ after 50 years.

With the increase in GMAT, the response of permafrost layers to external environmental thermal disturbances also strengthened. We analyzed the changes in ALT after 20 and 50 years under different GMAT conditions, as shown in Table 2.

**Table 2.** The increase in ALT under different GMAT conditions.

| $T_0$/°C | −0.5 | −1.0 | −1.5 | −2.0 | −2.5 | −3.0 | −3.5 | −4.5 | −5.5 |
|---|---|---|---|---|---|---|---|---|---|
| 20 years/m | 0.76 | 0.54 | 0.44 | 0.35 | 0.31 | 0.24 | 0.18 | 0.13 | 0.09 |
| 50 years/m | 1.60 | 1.35 | 1.13 | 0.92 | 0.81 | 0.69 | 0.58 | 0.48 | 0.43 |

According to Table 2, establishing the calculation formula between the increase of ALT and the initial GMAT after 20 and 50 years, as shown below:

$$\Delta D_1 = 0.848e^{0.4183T_0} \quad (7)$$

$$\Delta D_2 = 1.6808e^{0.2737T_0} \quad (8)$$

where $\Delta D_1$ represents the increase in ALT after 20 years; $\Delta D_2$ represents the increase in ALT after 50 years; $T_0$ is the initial GMAT. The goodness-of-fit $R^2$ of Equations (4) and (5) are 0.986 and 0.979, respectively, which can accurately predict the changes in ALT in the QTEC after 20 and 50 years.

## 3. Results

### *3.1. Prediction of Permafrost Thawing Settlement after 20 and 50 Years*

Based on the RBF neural networks prediction model of GMAT and ALT and the numerical model of GMAT and ALT growth under climate warming scenarios, the distribution of permafrost subgrade thawing depth and thawing settlement after 20 and 50 years was obtained. The calculation results are analyzed as follows.

3.1.1. Distribution of Subgrade Thawing Depth after 20 and 50 Years

Figure 3 shows the distribution maps of the GMAT and ALT after 20 and 50 years. It can be seen in Figure 3a that the permafrost in the QTEC will mainly be low-temperature and basically stable with GMAT between −2 °C and −1 °C within the next 20 years, and will be primarily distributed in the Kunlun Mountain, Kekexili Mountain, Beiluhe Basin, Fenghuo Mountain and Tanggula Mountain areas, with a small amount of distribution near the Buqu River Valley and the Chiqu Valley. In addition, high-temperature unstable permafrost (−1 °C to −0.5 °C) will be widely distributed, mainly in the Riachiqu River Basin, Chumar River Plain and Kaixinling Mountain area, with less distribution in the Tanggula Mountain and intermountain basins, and sporadic distribution near the Beilu River. Low-temperature stable permafrost (<−2 °C) is rarely distributed within the corridor, only in the Fenghuo Mountain and Kekexili Mountain areas, with sporadic distribution in the Kunlun Mountain area. The Gaerqu River Basin is mainly distributed with high-temperature extremely unstable permafrost (−0.5 °C to 0 °C), with a small distribution in the Chumar River Basin, Riachiqu River Basin and Tanggula Mountain area.

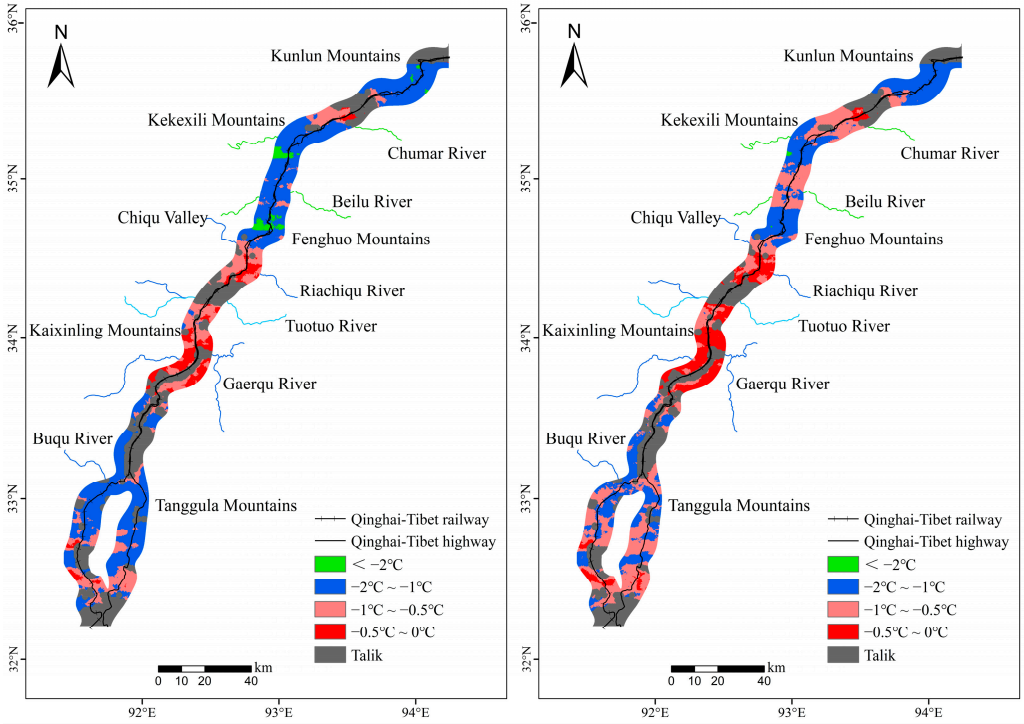



**Figure 3.** Ground mean annual temperature distribution map (**a**) after 20 years; (**b**) after 50 years.

From Figure 3b, it can be seen that the permafrost in the QTEC will mainly be high-temperature unstable permafrost (−1 °C to −0.5 °C) in the next 50 years. High-temperature unstable permafrost is widely distributed in the Chumar River Plain, Beiluhe Basin and Wuli Basin, with reduced distribution in the Kaixinling Mountain and Buqu River Valley. Low-temperature and basically stable permafrost (−2 °C~−1 °C) is mainly distributed in the Kunlun Mountain and Kekexili Mountain area, with less distribution in the Chumar River Plain, Buqu River Valley, Beiluhe Basin, Tanggula Mountain and intermountain basins. High-temperature extremely unstable permafrost (−0.5 °C to 0 °C) has a similar distribution to that expected in the next 20 years, mainly in the Gaerqu River Basin and Riachiqu River Basin, with a smaller distribution in the Chumar River and Tanggula Mountain and intermountain basins. Low-temperature stable permafrost (<−2 °C) will rarely be distributed within the corridor, and will only be found in the Kekexili Mountain area.

Overall, within both 20- and 50-year periods, the GMAT of permafrost in the QTEC shows an upward trend and regional permafrost exhibits a degradation trend. Correspondingly, the most significant areas are the Tanggula Mountain, the Chumar River Basin and the Beiluhe Basin, where permafrost degrades from low-temperature and basically stable permafrost to high-temperature unstable permafrost. In the Riachiru River Basin, Tuotuohe Basin and Gaerqu River Basin, the high-temperature unstable permafrost degrades to extremely high-temperature unstable permafrost.

The distribution map of ALT after 20 and 50 years is shown in Figure 4. As shown in Figure 4a, the ALT of permafrost in the QTEC will mainly be 3~5 m within the next 20 years, and will be mainly distributed south of the BeiluRiver, Fenghuo Mountain, Chiqu Valley, Buqu River Valley and Wenquan Faulted Basin, as well as in the Riachiqu River Basin. The ALT in the area north of the Beilu River is mainly 0~3 m, with the Kunlun Mountain area and Chumar River Plain mainly having an ALT of 0~2 m, with 2~3 m mainly distributed in the Beluhe Basin. Additionally, there will be a little distribution in the Kunlun Mountain, the Kekexili Mountain and Chumar River Plain. The ALT in Gairqu River Basin is expected to generally be above 5 m. In addition, the area of ALT above 5 m also has sporadic distribution in the Tanggula Mountain and intermountain basins, Buqu River Valley and Riachiqu River Basin.

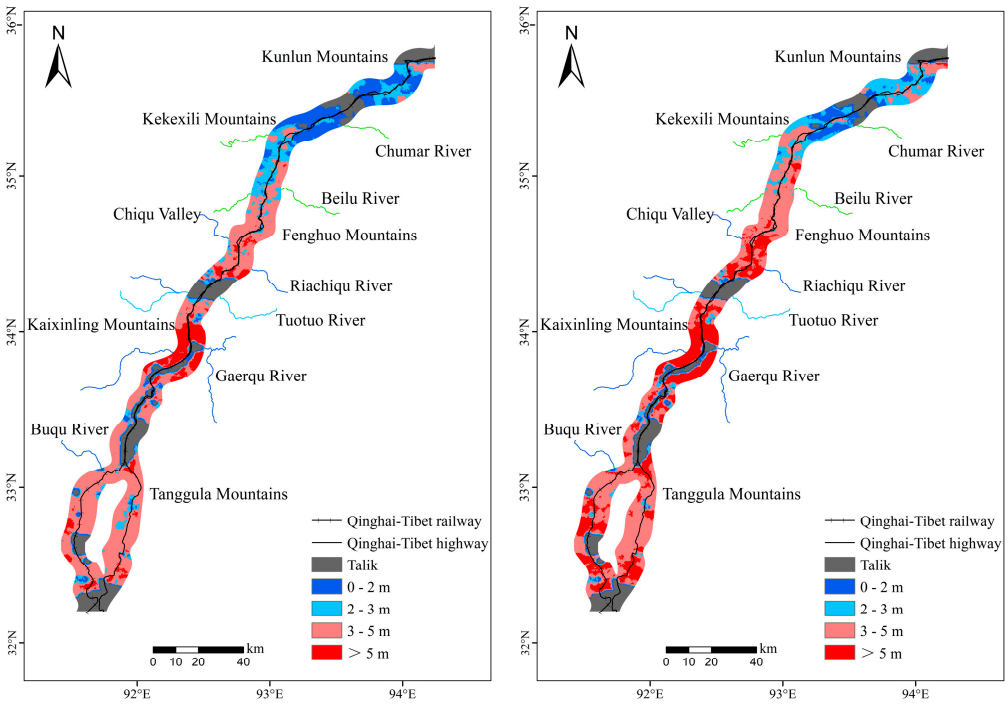



**Figure 4.** Active layer thickness distribution map (**a**) after 20 years; (**b**) after 50 years.

As shown in Figure 4b, the ALT of permafrost in the QTEC is mainly above 3 m. The area with an ALT of 3~5 m is slightly larger than that with an ALT above 5 m. The main areas with 3~5 m ALT are the Beiluhe Basin, Fenghuo Mountain area, and Chiqu Valley. In the Gaerqu River Basin and Riachiqu River Basin, the ALT is mainly above 5 m. Furthermore, an ALT above 5 m is also distributed in the Tanggula Mountain and intermountain basins, Wenquan Faulted Basin, Buqu River Valley and Kunlun Mountain area, basically covering the entire corridor. The area with an ALT below 3 m is mainly distributed in the Kunlun Mountain, Chumar River Plain, and Kekexili Mountain. Overall, for the next 20 and 50 years, the ALT of permafrost in the QTEC shows a similar increasing trend to GMAT. Among them, the most significant areas are the Gaerqu River Basin, Riachiqu River Basin, Tanggula Mountain and intermountain basin, with ALT increasing from 3~5 m to more

than 5 m. The ALT in some areas of the Beiluhe Basin, Kunlun Mountain Area, and Kekexili Mountain Area has increased from 2~3 m to 3~5 m. The ALT in the Chumar River Basin and Kunlun Mountain also increased from 0~2 m to 2~3 m.

Based on the GMAT and ALT, the subgrade thawing depth of the subgrade in the QTEC was calculated using Equation (2), then the distribution map of permafrost subgrade thawing depth in the study area after 20 and 50 years was obtained, as shown in Figure 5. It can be found that the permafrost subgrade thawing depth along the QTEC will mainly remain less than 9 m in the next 20 years, with only a few areas having 0~3 m thawing depths. The area with thawing depths of 6~9 m are expected to be slightly greater than the area with 3~6 m, and will mainly be distributed in the Kunlun Mountains, the Chumar River Plain, and the Kekexili Mountains. The area with a thawing depth of 6~9 m is mainly distributed in the Beiluhe Basin, Wenquan Faulted Basin, Tanggula Mountain and intermountain basins. In the Gaerqu River Basin and the Riachiqu River, the subgrade thawing depth is mainly above 9 m, and the areas with a subgrade thawing depth above 9 m are more widely distributed in the southern part of Tanggula Mountain and intermountain basins.

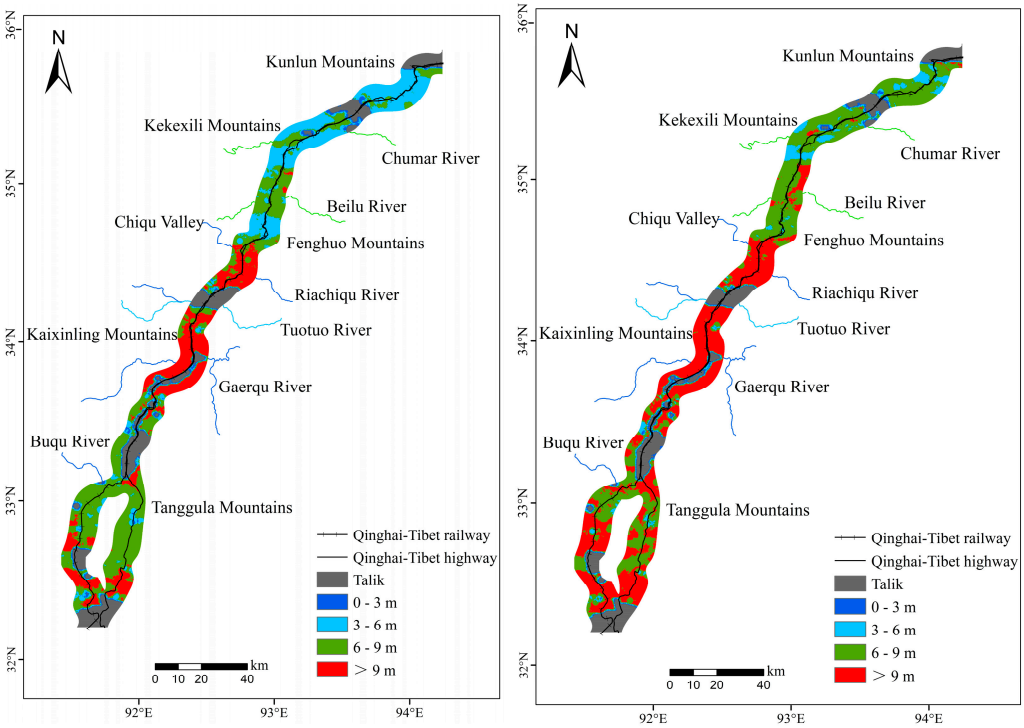



**Figure 5.** Subgrade thawing depth distribution map (**a**) after 20 years; (**b**) after 50 years.

According to Figure 5b, it can be seen that the subgrade thawing depth of permafrost in the QTEC will generally exceed 9 m in the next 50 years, with the bulk of the distribution being expected to occur in the Chiqu Valley, Wuli Basin, Kaixinling Mountain, Tongtianhe Basin, and Buqu River Valley. The subgrade thawing depth will usually be greater than 3 m, and we also anticipate a few areas with subgrade thawing depths of 3~6 m, which wull be distributed in the Kekexili Mountain, the Chumar River Plain and the Kunlun Mountain. The area with a subgrade thawing depth of 6~9 m is mainly distributed in the Beiluhe Basin, Kekexili Mountain Area and Chumar River Plain.

Overall, the permafrost subgrade thawing depth in the QTEC shows an increasing trend. Within the next 20 to 50 years, the subgrade thawing depth in the Chiqu Valley, Wuli Basin, Tongtianhe Basin, Tanggula Mountain and intermountain basins is expected to increase from 6~9 m to over 9 m. In addition, the subgrade thawing depth of above 9 m

in the Beiluhe Basin will exhibit significant expansion. Within this period, the subgrade thawing depth in the Fenghuo Mountain will basically increase to 6~9 m, and only a small part of the corridor will exhibit a subgrade thawing depth of 3~6 m.

#### 3.1.2. Distribution of Subgrade Thawing Settlement after 20 and 50 Years

The distribution map of permafrost subgrade thawing settlement for future 20 and 50 years is shown in Figure 6. In Figure 6a, it can be seen that the subgrade thawing settlement of permafrost in the QTEC after 20 years is expected to be between 0.02 m and 5.45 m, with an average value of about 0.93 m. The area with a subgrade thawing settlement over 1 m is mainly distributed throughout the entire corridor, mainly in the Chumar River Plain, Kunlun Mountains, Fenghuo Mountains, Gaerqu River Basin and near the Riachiqu River. In the Kekexili Mountain area, Chiqu Valley, Wenquan Faulted Basin and Buqu River Valley, the subgrade thawing settlement amount is mainly 0~0.25 m. There are relatively few areas with a subgrade thawing settlement of 0.25~1 m, among which the areas with a subgrade thawing settlement of 0.25~0.5 m are mainly located in the Kekexili Mountains, Chiqu Valley, Kaixinling Mountains and Tongtianhe Basin, and the area with a subgrade thawing settlement of 0.5~1 m is mainly distributed in the Kunlun Mountains, Chiqu Valley, Wuli Basin, Tanggula Mountain and intermountain Basins.

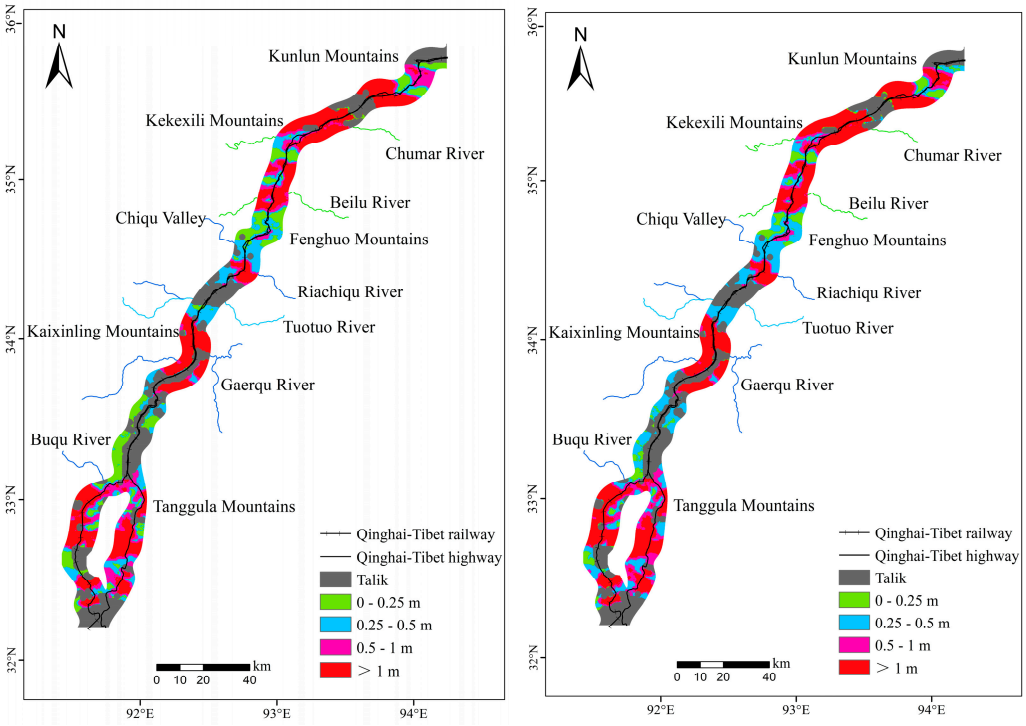



**Figure 6.** Subgrade thawing settlement distribution map (**a**) after 20 years; (**b**) after 50 years.

In Figure 6b, it can be seen that the permafrost subgrade thawing settlement along the QTEC in the next 50 years is expected to reach between 0.03 m and 6.21 m, with an average value of about 1.12 m. The distribution of subgrade thawing settlement is mainly above 1 m. The distribution of areas with a subgrade thawing depth of 0~0.25 m is relatively small, and is mainly observed in the Kunlun Mountains, Kekexili Mountains, Chiqu Valley, Tanggula Mountains and intermountain basins. In the Fenghuo Mountain, Wuli Basin, Tongtianhe Basin area and Wenquan Faulted Basin, the subgrade thawing settlement is mainly 0.25~0.5 m. Except for in the abovementioned areas, the subgrade thawing settlement in other areas is almost greater than 9 m, covering the entire corridor, especially in the Gaerqu River Basin, Chumar River Plain, and Beiluhe Basin. By comparison, when

considering the permafrost subgrade thawing settlement for next 20 and 50 years, it can be found that the permafrost thawing settlement in Kunlun Mountains, Fenghuo Mountains, Chiqu Valley, and Wenquan Faulted Basin is expected to increase from 0~0.25 m to 0.25~0.5 m. In addition, the area with a subgrade thawing settlement of over 9 m has been expanded and spread throughout the entire corridor.

### *3.2. Risk Zoning of Permafrost Subgrade Thawing Settlement after 20 and 50 Years*

Based on the previous research results, the risk of subgrade thawing settlement in QTEC is classified as follows: 0~0.1 m is low-risk, 0.1~0.5 m is medium-risk, 0.25~0.5 m is high-risk, and settlement exceeding 0.5 m represents a significant risk [29]. Utilizing this criterion, a risk zoning map depicting the projected permafrost subgrade thawing settlement in the QTEC for the next 20 and 50 years was calculated, as shown in Figure 7.

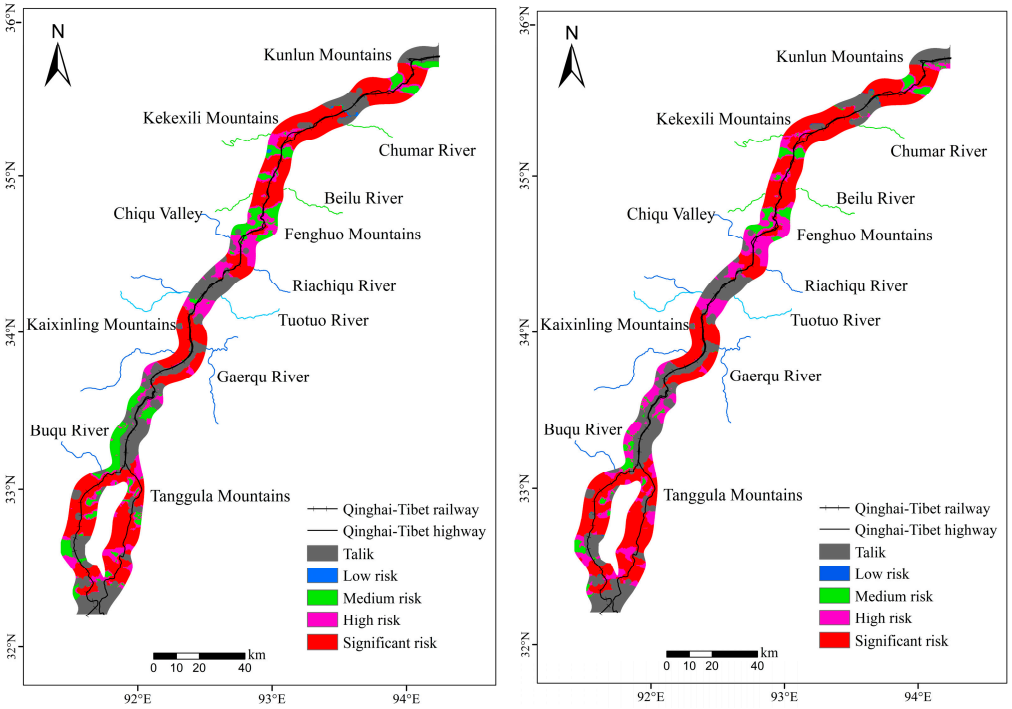



**Figure 7.** Subgrade thawing settlement risk distribution map (**a**) after 20 years; (**b**) after 50 years.

It can be seen that the risk of permafrost subgrade thawing settlement in the QTEC is mainly expected to become a significant risk in the next 20 years. There are few projected low-risk areas within the QTEC, with only a small portion distributed in the Chumar River Plain and the Kekexili Mountain Area. The medium-risk areas are mainly distributed in Fenghuo mountainous areas, Chiqu Valley, Wenquan Faulted Basin and Touerjiu Mountains. In the Kunlun Mountains, Kekexili Mountains, Beiluhe Basin, Kaixinling Mountains and Buqu River Valley; there is also a small distribution of medium risk. In the Wuli Basin, Tuotuohe Basin, Kaixinling Mountain Area and Buqu River Valley, the risk of subgrade thawing settlement is mainly higher. When looking at the 50-year projections, it can be seen that the area of significant risk has obviously increased. Compared to the risk of subgrade thawing settlement in the next 20 years, the scope of the high-risk areas in Tanggula Mountain and intermountain basins has significantly increased. Meanwhile, the medium-risk areas in the Kunlun Mountains, Wenquan Fault Basin, Chiqu Valley and Buqu Valley have transformed into high-risk areas, and the risk of subgrade thawing settlement has further increased.

In order to further analyze the distribution of various types of permafrost subgrade thawing settlement risks in the QTEC after 20 and 50 years, the corresponding areas and proportions of various risk levels were calculated, as shown in Figure 8.

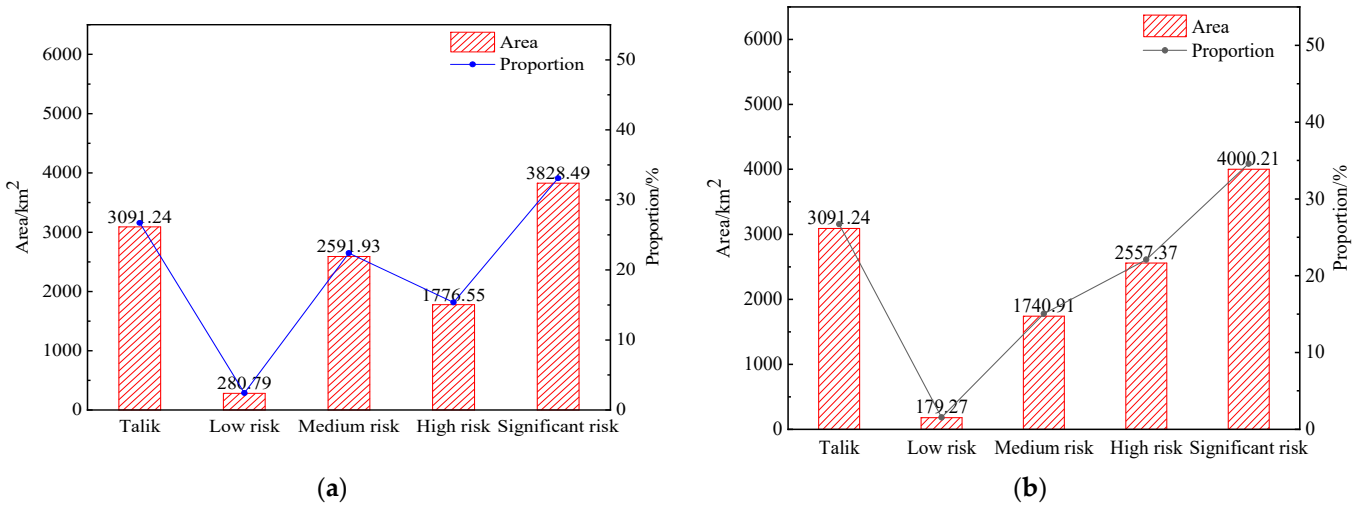
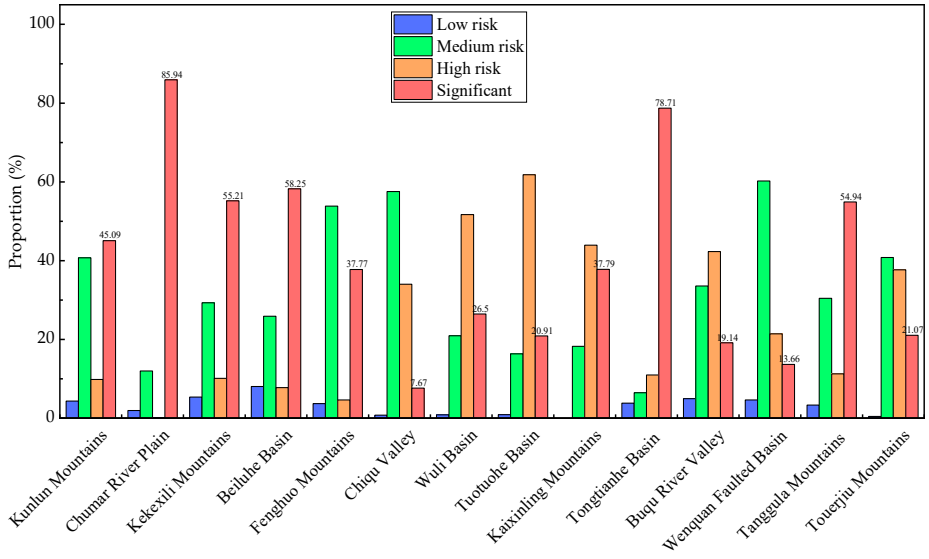


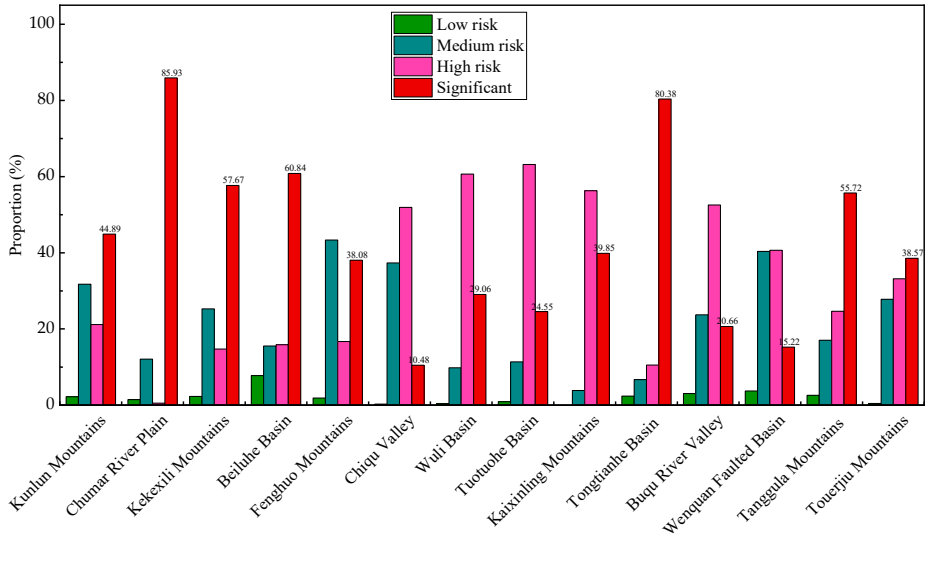

**Figure 8.** The areas and proportions of various subgrade thawing settlement risk (**a**) after 20 years; (**b**) after 50 years.

According to Figure 8a, it can be seen that the subgrade thawing settlement risk of permafrost in the QTEC after 20 years represents the most significant risk, with an area of 3828.49 km$^2$, accounting for 26.72%, which is mainly distributed in the Chumar River Plain, Beiluhe Basin, and Tongtianhe Basin. The area of medium risk is 2591.93 km$^2$, accounting for 22.4% of the total area, and this is mainly distributed in Fenghuo mountainous areas, Chiqu Valley and Wenquan Fault basin. The areas with high subgrade thawing settlement risk are mainly distributed in the Wuli Basin, Tuotuohe Basin, Kaixinling Mountain Area and Buqu River Valley, with an area of 1776.55 km$^2$, accounting for 15.36% of the total area. The low-risk area is 280.79 km$^2$, accounting for 2.43%. Compared with the risk distribution in next 20 years, it can be seen in Figure 8b that the permafrost subgrade thawing settlement risk in the QTEC after 50 years is also mostly considered to be at significant risk, with the area increasing to 4000.21 km$^2$, accounting for 34.58%. Both low-risk and medium-risk areas have decreased, with low-risk areas decreasing to 179.27 km$^2$, accounting for 1.55%, and medium risk areas decreasing to 1740.91 km$^2$, accounting for 15.05% of the total area. The high-risk area has significantly increased to 2557.37 km$^2$, accounting for 22.1% of the total area.

We divided the Qinghai–Tibet Project Corridor into 14 sections, and the area and the proportion of various risk levels in different areas are shown in Figure 9. It can be seen that, for both the next 20 and the next 50 years, the Kunlun Mountains, Chumar River Plain, Kekexili Mountains, Beiluhe Basin and Tongtianhe Basin are mainly categorized as significant-risk areas, and the proportion of significant-risk areas in most sections exceeds half of the total area. For the next 50 years, among the 14 sections along the QTEC, only Fenghuo mountainous area has a medium risk of subgrade thawing settlement; the proportion of low- and medium-risk areas has decreased, and the high-risk and significant-risk areas have significantly increased. For the next 20 years to 50 years, the low-risk and medium-risk areas have decreased, while the high-risk areas have increased. This provides further indication that the risk of permafrost subgrade thawing settlement along the QTEC cumulatively increases over time.




(**a**)




(**b**)

**Figure 9.** The proportion of various subgrade thawing settlement risks in 14 regions (**a**) after 20 years later; (**b**) after 50 years.

The GMAT and ALT are two important factors reflecting the occurrence characteristics of permafrost and have a significant effect on the risk ranking of subgrade thawing settlement. Thus, the average GMAT and ALT under different thawing settlement risk levels over the next 20 and 50 years were analyzed, respectively, as shown in Figure 10. It can be seen that, as the risk level increases from low-risk to medium-risk and high-risk, the average values of GMAT and ALT show a gradual increasing trend. It is noted that the GMAT and ALT indexes have strong correlation with subgrade thawing settlement risk. However, when the subgrade thawing settlement risk reaches a significant level, the corresponding average values of GMAT and ALT exhibit a sharply decreasing trend. It can be inferred that the subgrade permafrost thawing settlement risk is not solely determined by GMAT and ALT; other factors, such as permafrost ice content distribution, also have a certain influence.

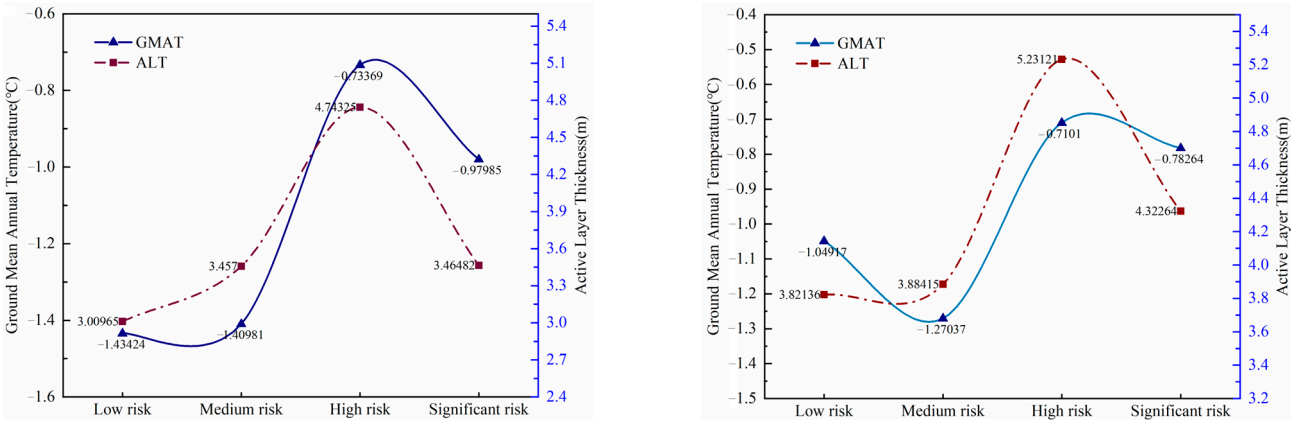



**Figure 10.** Average ground mean annual temperature and active layer thickness at four thawing settlement risks (**a**) after 20 years; (**b**) after 50 years.

## 4. Conclusions

In present work, we established a prediction model for 26 m width subgrade thawing settlement in the QTEC considering the climate warming effect. The distribution characteristics of thawing settlement over the next 20 and 50 years were obtained and analyzed. The conclusions are as follows:

(1) As a result of climate warming, the thawing depth and settlement of 26 width permafrost subgrade in the QTEC will increase rapidly. The permafrost thawing depth will be mainly below 9 m in the next 20 years, and the permafrost thawing depth will almost always exceeds 9 m within the next 50 years. The subgrade thawing settlement along the QTEC will be between 0.02 m and 5.45 m, with an average value of 0.93 m after a 20-year period. Meanwhile, the subgrade thawing settlement will mainly surpass 1.0 m after a 50-year period, and is expected to spread throughout the entire corridor.

(2) The thawing settlement risks of permafrost subgrade in the QTEC in the next 20 and 50 years will mainly be significant risks, with an area and proportion of 3828.49 $km^2$ and 26.72% and 4000.21 $km^2$ and 34.58%, respectively. However, the areas of low and medium risk are expected to drastically reduce at the same time, and are expected to only account for 1.55% and 15.05% after 50 years. The significant-risk areas within the next 50 years will be mainly distributed in the Kunlun Mountains, Chumar River Plain, Kekexili Mountains, Tongtianhe Basin, Tanggula Mountains and intermountain basins.

(3) In view of the large-scale, high-risk permafrost subgrade thawing settlement that will appear in the future, it is recommended to strengthen targeted ground temperature monitoring and disease investigation and adopt measures such as roadbed replacement, cooling or insulation of special subgrade structures, or separate subgrade structures for serious engineering disease sections.

**Author Contributions:** Conceptualization, J.L. and Y.Z. (Yue Zhai); methodology, X.L.; software, F.C. and J.L.; validation, Y.Z. (Yue Zhai), J.L., and J.C.; formal analysis, X.L. and Y.Z. (Yu Zhu); investigation, Y.Z. (Yue Zhai); resources, F.C. and Y.Z. (Yue Zhai); data curation, J.L. and Y.Z. (Yu Zhu); writing—original draft preparation, J.L.; writing—review and editing, J.L. and Y.Z. (Yue Zhai). All authors have read and agreed to the published version of the manuscript.

**Funding:** This research was funded by the National Science Foundation of China (Grant No. 42371149, 42230712), the Natural Science Foundation of Shaanxi Province (Grant No. 2022JM-143), the Innovation Capacity Support Plan Project of Shaanxi Province (Grant No. 2021TD-55, 2022KXJ-107), the open fund of National Key Laboratory of Green and Long-Life Road Engineering in Extreme Environment (YGY2021KFKT03), and the Scientific Innovation Practice Project of Postgraduates of Chang'an University (300103723048). We are grateful to the anonymous reviewers for their constructive comments to improve this manuscript.

**Institutional Review Board Statement:** Not applicable.

**Informed Consent Statement:** Not applicable.

**Data Availability Statement:** The data are available in the case that they are required.

**Conflicts of Interest:** The authors declare no conflicts of interest. Jianbing Chen is employee of National Key Laboratory of Green and Long-Life Road Engineering in Extreme Environment, CCCC First Highway Consultants Co. Ltd. The paper reflects the views of the scientists and not the company.

## References


1. Cao, B.; Zhang, T.J.; Wu, Q.B.; Sheng, Y.; Zhao, L.; Zou, D.F. Permafrost zonation index map and statistics over the Qinghai-Tibet Plateau based on field evidence. *Permafr. Periglac. Process. J.* **2019**, *30*, 178–194. [CrossRef]
2. Chen, J.; Dang, H.M.; Mei, Q.H. Settlement disease of pile foundation of dry bridge in perennial permafrost area of Qinghai-Tibet Railway and its management revelation. *J. Glaciol. Geocryol.* **2023**, *45*, 1327–1334.
3. Wang, Z.; Zhang, H.J.; Peng, H. Engineering capacity analysis and ease of construction zoning evaluation of Qinghai-Tibet engineering corridor. *Highway* **2023**, *68*, 304–312.
4. Cui, F.Q.; Zhu, Y.; Liu, X.N. Characteristics and Influence Rules of Roadside Ponding along the Qinghai–Tibet Highway. *Water* **2024**, *16*, 954. [CrossRef]
5. Zhang, S.Z.; Niu, F.J.; Wang, J.C. Evaluation of Damage Probability of Railway Embankments in Permafrost Regions in Qinghai-Tibet Plateau. *Eng. Geol.* **2021**, *284*, 106027. [CrossRef]
6. Gao, X.J.; Shi, Y.; Zhang, D.F.; Giorgi, F. Climate change in China in the 21st century as simulated by a high resolution regional climate model. *Chin. Sci. Bull.* **2012**, *57*, 1188–1195. [CrossRef]
7. Cheng, G.D.; He, P. Linear engineering construction in permafrost areas. *J. Glaciol. Geocryol.* **2001**, *23*, 213–217.
8. Wang, Z.J. Permafrost Engineering Problems in the Construction of the Qinghai-Tibet Railway. *Chin. Railw.* **2002**, *10*, 31–37. [CrossRef]
9. O'Neill, H.B.; Smith, S.L.; Burn, C.R. Widespread permafrost degradation and thaw subsidence in northwest Canada. *J. Geophys. Res. Earth Surf.* **2023**, *128*, e2023JF007262. [CrossRef]
10. Deng, X.; Pan, S.; Wang, Z. Application of the Darcy-Stefan model to investigate the thawing subsidence around the wellbore in the permafrost region. *Appl. Therm. Eng.* **2019**, *156*, 392–401. [CrossRef]
11. Chen, W.X.; Guo, J.L. Field monitoring of railroad foundation settlement in permafrost zone. *Subgrade Eng.* **2022**, *40*, 24–58. [CrossRef]
12. Guo, J.L. A prediction model of subgrade settlement of Qinghai-Tibet Railway based on gray BP neural network. *Chin. Railw.* **2022**, *30*, 63–68. [CrossRef]
13. Wang, S.L. Characteristics of Permafrost Degradation and Settlement Prediction of the Foundation of Beihei Highway. Master's Thesis, Northeast Forestry University, Harbin, China, 2021.
14. Zaretskii, Y.K. Scientific Legacy of NA Tsytovich. *Soil Mech. Found. Eng.* **2000**, *37*, 131–139. [CrossRef]
15. Sun, Z.; Zhao, L.; Hu, G.J. Numerical Simulation of Thaw Settlement and Permafrost Changes at Three Sites Along the Qinghai-Tibet Engineering Corridor in a Warming Climate. *Geophys. Res. Lett.* **2022**, *49*, e2021GL097334. [CrossRef]
16. Ni, J.; Wu, T.H.; Zhu, X.F. Risk Assessment of Potential Thaw Settlement Hazard in the Permafrost Regions of Qinghai-Tibet Plateau. *Sci. Total Environ.* **2021**, *776*, 145855. [CrossRef]
17. Zhang, Y.; Chen, W.J.; Riseborough, W.D. Transient projections of permafrost distribution in Canada during the 21st century under scenarios of climate change. *Glob. Planet. Chang.* **2007**, *60*, 443–456. [CrossRef]
18. Alexander, N.F. A route to understanding the variability in permafrost distribution under climate change. *Adv. Clim. Chang. Res.* **2023**, *14*, 164–165.
19. Huang, S.; Ding, Q.; Chen, K.Z. Changes in Near Surface Permafrost Temperature and Active Layer Thickness in Northeast China in 1961—2020 Based on GIPL Model. *Cold Reg. Sci. Technol.* **2023**, *206*, 103709. [CrossRef]
20. Hong, E.; Perkins, R.; Trainor, S. Thaw Settlement Hazard of Permafrost Related to Climate Warming in Alaska. *Arctic* **2014**, *67*, 93–103. [CrossRef]
21. Ruan, G.F.; Zhang, J.M.; Chai, M.T. Study on the risk zoning of thaw and subsidence disaster in the Qinghai-Tibet engineering corridor under climate change scenario. *J. Glaciol. Geocryol.* **2014**, *36*, 811–817.
22. Zhao, Y. Assessment of Thawing Infiltration and Ground Subsidence of High-Temperature Permafrost under Long-Term Climate Change. Master's Thesis, Heilongjiang University, Harbin, China, 2021. [CrossRef]
23. Rodenhizer, H.; Ledman, J.; Mauritz, M. Carbon thaw rate doubles when accounting for subsidence in a permafrost warming experiment. *J. Geophys. Res. Biogeosci.* **2020**, *125*, e2019JG005528. [CrossRef]
24. Zhang, Z.Q.; Wu, Q.B. Predicted changes in active permafrost layer thickness on the Tibetan Plateau under climate change scenarios. *J. Glaciol. Geocryol.* **2012**, *34*, 505–511.
25. Xu, X.M.; Wu, Q.B. Characterization of changes in the thickness of the active layer of permafrost at the source of the Sanjiang River. *J. Glaciol. Geocryol.* **2024**, *46*, 1–15.

26. Nan, Z.T.; Li, S.X.; Cheng, G.D. Scenarios of permafrost changes on the Qinghai-Tibetan Plateau in the next 50 and 100 years. *Sci. China (Ser. D Earth Sci.)* **2004**, *34*, 528–534.
27. Wei, D.; Zhao, T.H.; Mu, Y.H. Study on the geothermal process of perennial permafrost and thaw zone in the Tuotuohe Basin under the background of climate warming. *J. Glaciol. Geocryol.* **2022**, *44*, 427–436.
28. Bai, R.Q.; Lai, Y.M.; Zhang, M.Y. Investigating the thermo-hydro-mechanical behavior of loess subjected to freeze–thaw cycles. *Acta Geotech.* **2024**, *19*, 1–14. [CrossRef]
29. Bai, R.Q.; Lai, Y.M.; Pei, W.S. Study on the frost heave behavior of the freezing unsaturated silty clay. *Cold Reg. Sci. Technol.* **2022**, *197*, 103525. [CrossRef]
30. Zhang, J.M. Research on the Stability of Frozen Soil Subgrades in the Qinghai Tibet Plateau and the Classification of Permafrost in Highway Engineering. Doctoral Thesis, Institute of Environment and Engineering in Cold and Dry Regions, Chinese Academy of Sciences, Beijing, China, 2004.
31. Liu, Z.Y.; Zhu, Y.; Chen, J.B.; Cui, F.Q. Risk Zoning of Permafrost Thaw Settlement in the Qinghai–Tibet Engineering Corridor. *Remote Sens.* **2023**, *15*, 3913. [CrossRef]
32. Liu, Z.Y.; Cui, F.Q.; Chen, J.B. Study on the permafrost heat transfer mechanism and reasonable interval of separate embankment for the Qinghai-Tibet expressway. *Cold Reg. Sci. Technol.* **2019**, *170*, 102952. [CrossRef]
33. Zhu, Z.Y.; He, Z.H.; Luo, F. Evaluating the performance of a novel ventilated embankment structure in warm permafrost regions by numerical simulation. *Cold Reg. Sci. Technol.* **2023**, *209*, 103805. [CrossRef]
34. Taylor, G.S.; Luthin, J.N. A model for Coupled Heat and Moisture Transfer during Soil Freezing. *Can. Geotech. J.* **1978**, *15*, 548–555. [CrossRef]
35. Liu, Z.Y.; Chen, J.B.; Jin, L.; Zhang, Y.J.; Lei, C. Roadbed temperature study based on earth-atmosphere coupled system in permafrost regions of the Qinghai-Tibet Plateau. *Cold Reg. Sci. Technol.* **2013**, *86*, 167–176. [CrossRef]
36. Liu, Z.Y.; Wang, S.W.; Jiang, Z.Y.; Dong, Y.H.; Chen, J.B.; Cui, F.Q. Study on the coupling thermal effect of thermokarst lake and high sunny slope on permafrost embankment. *Transp. Geotech.* **2023**, *41*, 101024. [CrossRef]


**Disclaimer/Publisher's Note:** The statements, opinions and data contained in all publications are solely those of the individual author(s) and contributor(s) and not of MDPI and/or the editor(s). MDPI and/or the editor(s) disclaim responsibility for any injury to people or property resulting from any ideas, methods, instructions or products referred to in the content.